# Quarterly Progress Report

Period of Performance:

**January 1–March 31, 2006**

**Prepared by:**

**Dr. Kuo-Ta Hsieh**
**Principal Investigator**

**Institute for Advanced Technology**
**The University of Texas at Austin**
**3925 W. Braker Ln., Suite 400**
**Austin, TX 78759**

**Grant #: N00014-05-1-0588**

Distribution: Electronic and US Mail
Recipients: Stephen. C. Schreppler, ONR 334
Julia M. Gallmon, ONR N66018
DTIC
NRL Code 5227
G. Olivas, ONR

Approved for public release; distribution unlimited

IAT.R 0455

# REPORT DOCUMENTATION PAGE

Form Approved
OMB NO. 0704-0188



| 1. AGENCY USE ONLY (Leave blank) | 2. REPORT DATE | 3. REPORT TYPE AND DATES COVERED |
|---|---|---|
| | May 2006 | Quarterly Report, 01/01–03/31/2006 |

4. TITLE AND SUBTITLE

Quarterly Progress Report: Modeling and Simulation of the Homopolar Motor Test Apparatus

5. FUNDING NUMBERS

Contract # N00014-1-0588

6. AUTHOR(S)

K.-T. Hsieh

7. PERFORMING ORGANIZATION NAME(S) AND ADDRESS(ES)

Institute for Advanced Technology
The University of Texas at Austin
3925 W. Braker Lane, Suite 400
Austin, TX 78759-5316

8. PERFORMING ORGANIZATION REPORT NUMBER

IAT.R 0455

9. SPONSORING / MONITORING AGENCY NAME(S) AND ADDRESS(ES)

Office of Naval Research Regional Office San Diego
4520 Executive Drive STE 300
San Diego CA 92121-3019

10. SPONSORING / MONITORING AGENCY REPORT NUMBER

11. SUPPLEMENTARY NOTES

12a. DISTRIBUTION / AVAILABILITY STATEMENT

Approved for public release; distribution unlimited.

12b. DISTRIBUTION CODE

A

13. ABSTRACT *(Maximum 200 words)*

The US Navy is in the advanced stages of developing a superconducting homopolar motor/generator (SCHPMG) machine for ship propulsion. Electrical contact (brush/slip ring) performance is a limiting factor in SCHPMG technology development. Experimental evidence has shown that brush wear is not only highly asymmetric among brushes of opposite polarity (anode and cathode) but is also non-uniform within the contact area of the individual brush. This asymmetric and non-uniform wearing has limited the life and efficiency of the brush assembly, and debris from worn brushes can adversely affect the machine operating environment. Accurate EM characterization of the brush/rotor or brush/slip ring interface is essential not only for understanding the wear behavior of the brush but also for optimal brush design.

14. SUBJECT TERMS

superconducting homopolar motors, inhomogenous brush wear, polarity dependence, destabilized force

15. NUMBER OF PAGES

11

16. PRICE CODE

| 17. SECURITY CLASSIFICATION OF REPORT | 18. SECURITY CLASSIFICATION OF THIS PAGE | 19. SECURITY CLASSIFICATION OF ABSTRACT | 20. LIMITATION OF ABSTRACT |
|---|---|---|---|
| Unclassified | Unclassified | Unclassified | UL |

NSN 7540-01-280-5500

Standard Form 298 (Rev.2-89)
Prescribed by ANSI Std. 239-18 298-102

**QUARTERLY PROGRESS SUMMARY REPORT**
**Period reported: January 1 through March 31, 2006**

## 1. Contract Summary

- Grant number: N00014-05-1-0588
- Period of performance: April 1, 2005 to September 30, 2006
- Total value of awarded grant: $481,000.00

## 2. Contract Personnel

The key personnel involved in this effort are Dr. Kuo-Ta Hsieh, Principal Investigator, and Dr. Sikhanda Satapathy. Dr. Hsieh is a research scientist at the Institute for Advanced Technology (IAT) of The University of Texas at Austin (UT) and co-team leader for the Analysis and Code Development Section of the Electromagnetic Systems Division (ESD). He is an expert on the development of high-capability electromechanical codes and advanced computing. Dr. Hsieh is the sole author of the advanced electromechanical code EMAP3D, a major code used in this effort. Dr. Satapathy is a research scientist at IAT and co-team leader of the Analysis and Code Development Section of ESD. His expertise is in structural analysis and mechanical design. He focuses on mechanical simulations and the improvement of brush design for better performance. Mr. Cody Hammock, a research associate at IAT, constructs the electromagnetic (EM) models of the motors and performs EM simulations.

## 3. Technical Report

### *3.1. Background*

The US Navy is in the advanced stages of developing a superconducting homopolar motor/generator (SCHPMG) machine for ship propulsion. Electrical contact (brush/slip ring) performance is a limiting factor in SCHPMG technology development. At the interface between brush and slip ring, where current transfer occurs, factors that will affect wear include the current density distribution $j$, local magnetic field $B$, temperature, and EM forces as the brush slides with velocity $v$ on an imperfect rotor surface. Experimental evidence has shown that brush wear is not only highly asymmetric among brushes of opposite polarity (anode and cathode) but is also non-uniform within the contact area of the individual brush. This asymmetric and non-uniform wearing has limited the life and efficiency of the brush assembly, since the full volume of brush fiber material is not fully utilized, and debris from worn brushes can adversely affect the machine operating environment, ultimately possibly leading to internal short circuits (arc-over). Accurate EM characterization of the brush/rotor or brush/slip ring interface is essential not only for understanding the wear behavior of the brush but also for optimal brush design.

### *3.2. Modeling*

Two half-symmetrical finite element models, shown in Figures 1a and 1b, with aspect ratios of 1:2 and 1:3 respectively, were constructed to study the effects of brush aspect ratio and packing factor on destabilized EM force, in order to obtain the optimum brush configuration. The models have eight stators, consisting of a field coil, a slip ring, brushes, and buses. The brush contact area is kept constant (2 $cm^2$). A transport current of 325 A is applied to each brush, and the field

coil current of 1.64 E6 ampere-turns is applied to produce the magnetic fields of 0.4 T at the brushes' locations. Thermally coupled electromagnetic simulations were conducted. The local adiabatic condition was assumed, and only bulk ohmic heating was considered in the simulations. The temperature-dependent electrical conductivity used is shown in Figure 2. The steady-state solution is reached at about 1.0 s. The results for the aspect ratio 1:3 model are shown in Figures 3–13. The end view of the field coil's current-density distributions is shown in Figure 3. The end view of current density distribution of the slip ring, brushes, and buses at 0.25 s and 1.0 s are shown in Figures 4 and 5, respectively. At 0.25 s, the transient eddy current due to the field coil current dominated. Any axial imbalance force due to asymmetric structure should occur during the field coil's energizing. The eddy current decays out at 1.0 s, and brush transport current remains. From Figure 5, the circumferential components of current densities are in opposite directions at the leading and trailing edges. These components of current densities interacting with the axial magnetic field could produce loads opposite to the radial direction, which tend to destabilize the brush. Figure 6 shows the 3D view of current flow at 1.0 s. The magnetic field distribution at 1.0 s is plotted in Figure 7. As expected, the radial component of magnetic field is the dominant component. A 3D view of body-force distribution on the slip ring, brushes, and buses at 1.0 s is shown in Figure 8. The detailed view of body-force distribution on one particular brush at 1.0 s is shown in Figure 9. It shows that the radial forces are in opposite directions at the leading and trailing edges, with a peak value of about 3.30 E5 $N/m^3$. The temperature distributions on the brush and slip ring at 1 sec and at 4 h are shown in Figures 10–13, respectively. The results for an aspect ratio of 1:2 are shown in Figures 14–17. Figures 14 and 15 show the body-force distribution of brushes at 1.0 s; the peak value is about 4.31 E5 $N/m^3$. Temperature distributions on the brushes and slip ring at 1.0 s are shown in Figures 16 and 17.

### *3.3 Conclusion*

Some conclusions can be drawn from these simulations, as follows:

- A fully postulated brush tends to reduce the destabilizing (radial) force.
- A brush with a high aspect ratio experiences less destabilizing force.
- Power loss per brush due to bulk ohmic heating is about 0.74 W for an aspect ratio of 1:2 vs. 0.72 watts for an aspect ratio of 1:3.
- Frictional heating is about 16.5 W per brush, based on 2 psi contact pressure and 12 m/s tip speed.
- Power loss per slip ring due to bulk ohmic heating is about 0.98 W for an aspect ratio of 1:2 vs. 0.9 watts for an aspect ratio of 1:3.

### *3.3 Future Work*

To continue the basic science study of brush/slip ring contact and the development of models of the brush/slip ring contact interface, the following is planned:

- Continue thermally coupled EM simulation to calculate the brush temperature distribution of the subscale motor, including the effects of motion, frictional heating, contact resistive heating, and cooling.

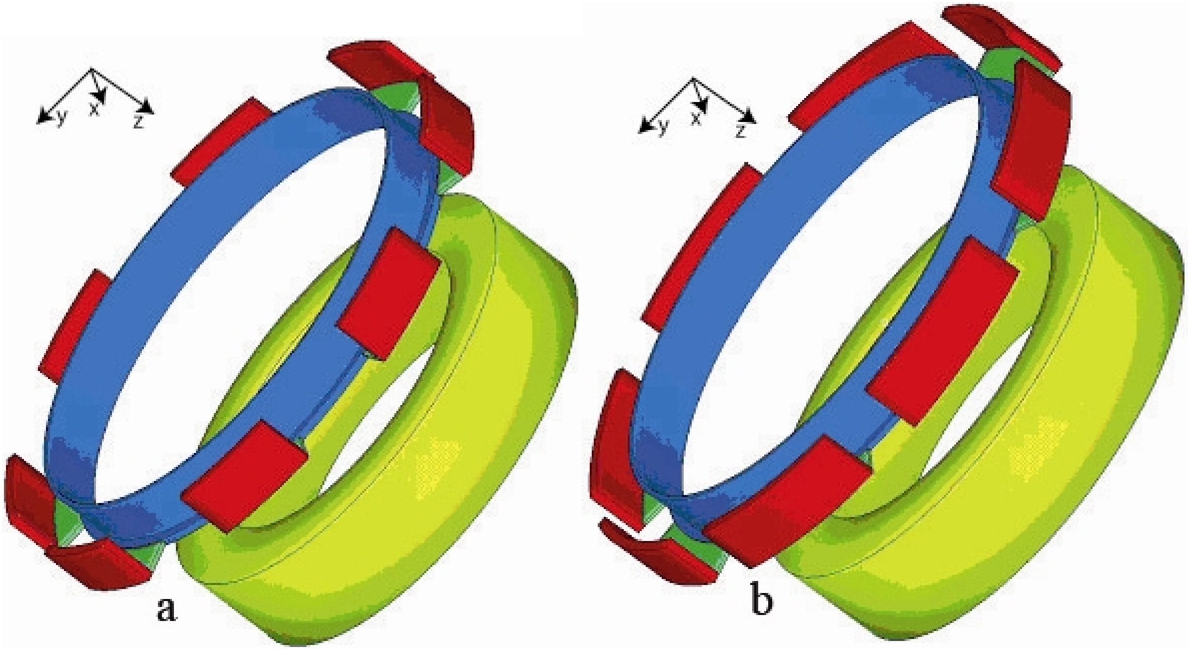


**Figure 1. a) Half symmetric FE model for aspect ratio 1:2. b) Half symmetric FE model for aspect ratio 1:3.**

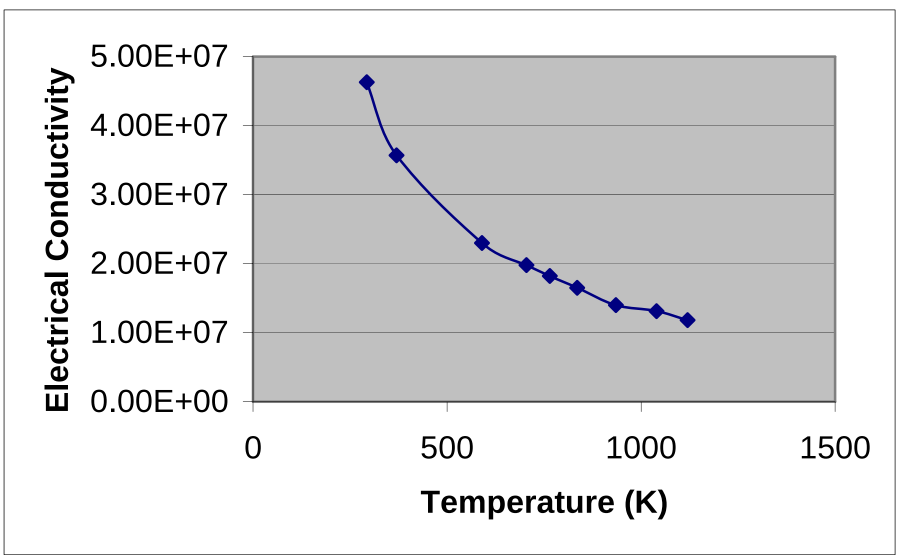


**Figure 2. Temperature-dependent electrical conductivity.**

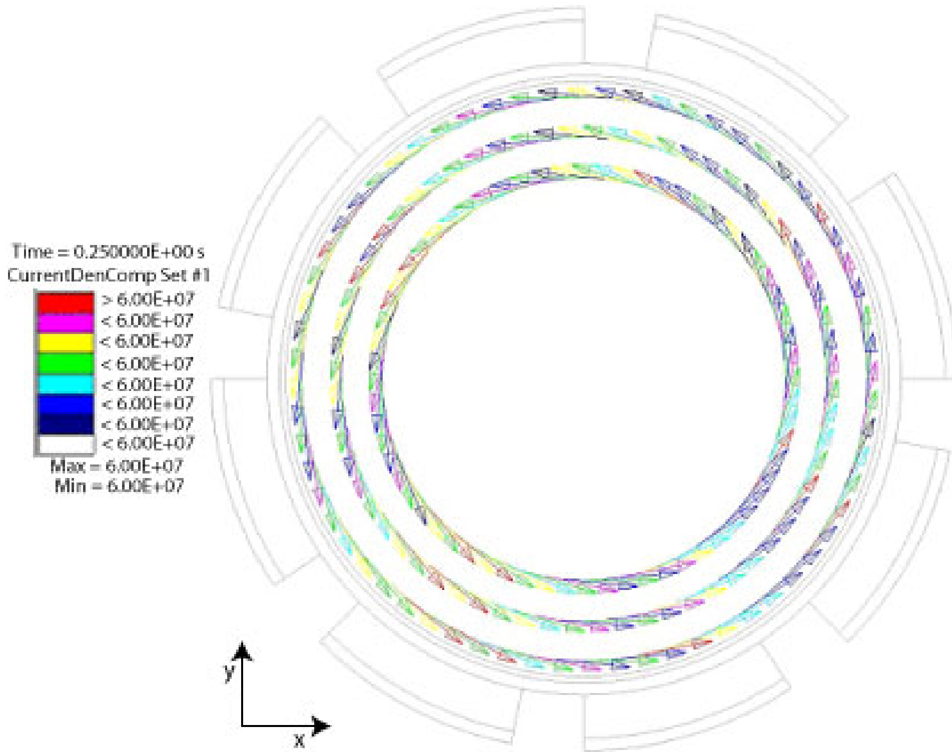


**Figure 3. Field coil current density for aspect ratio 1:3.**

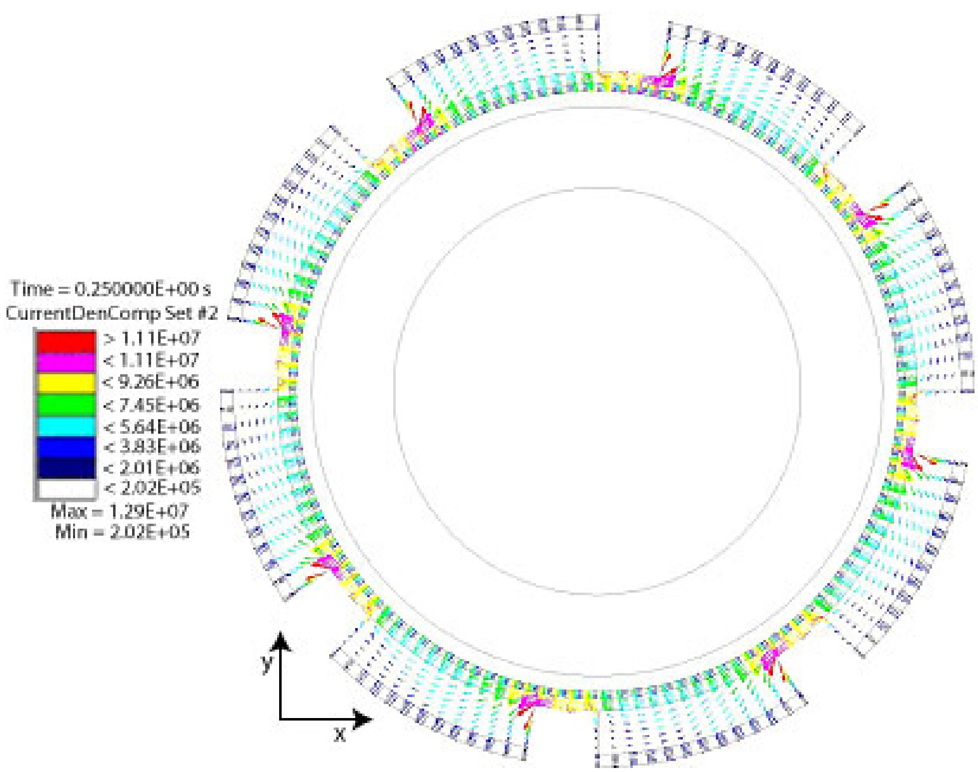


**Figure 4. End view of current densities on a slip ring, brushes, and buses at 0.25 s for aspect ratio 1:3.**

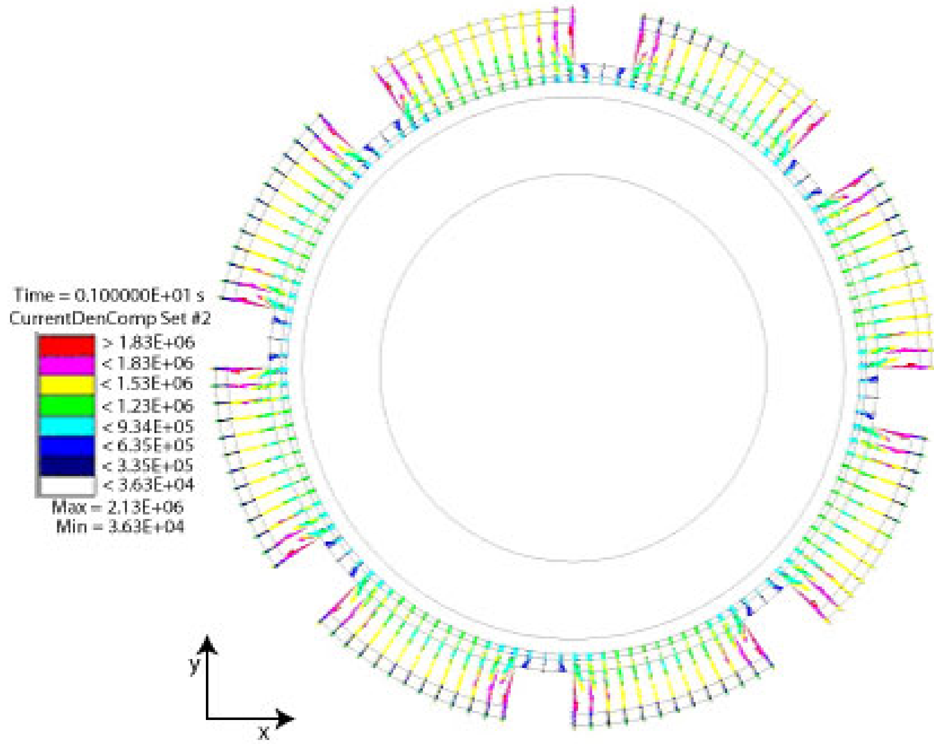


**Figure 5. End view of current densities on a slip ring, brushes, and buses at 1.0 s for aspect ratio 1:3.**

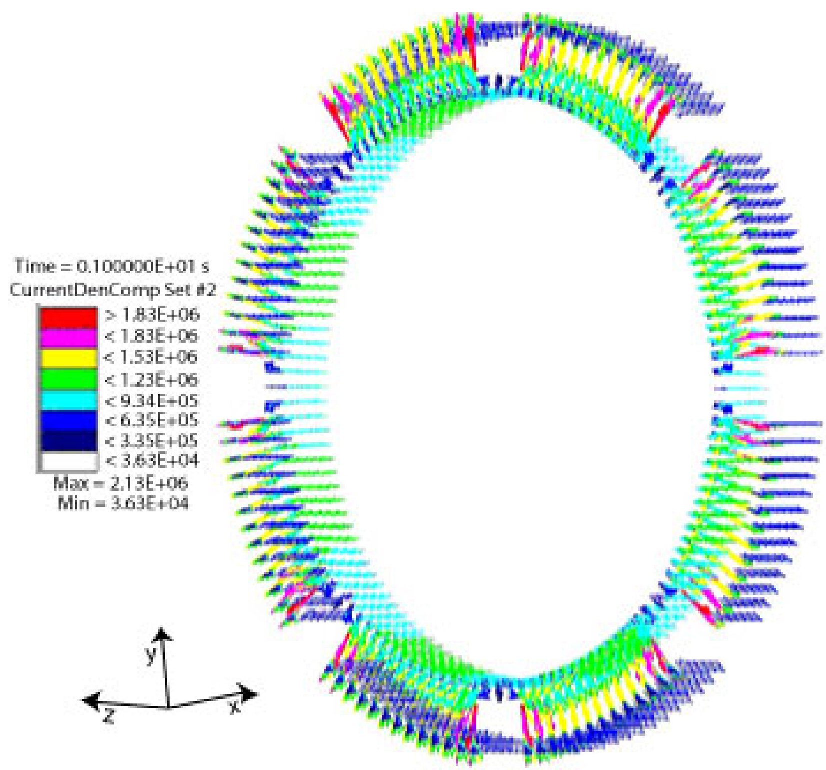


**Figure 6. 3D view of current densities on a slip ring, brushes, and buses at 1.0 s for aspect ratio 1:3.**

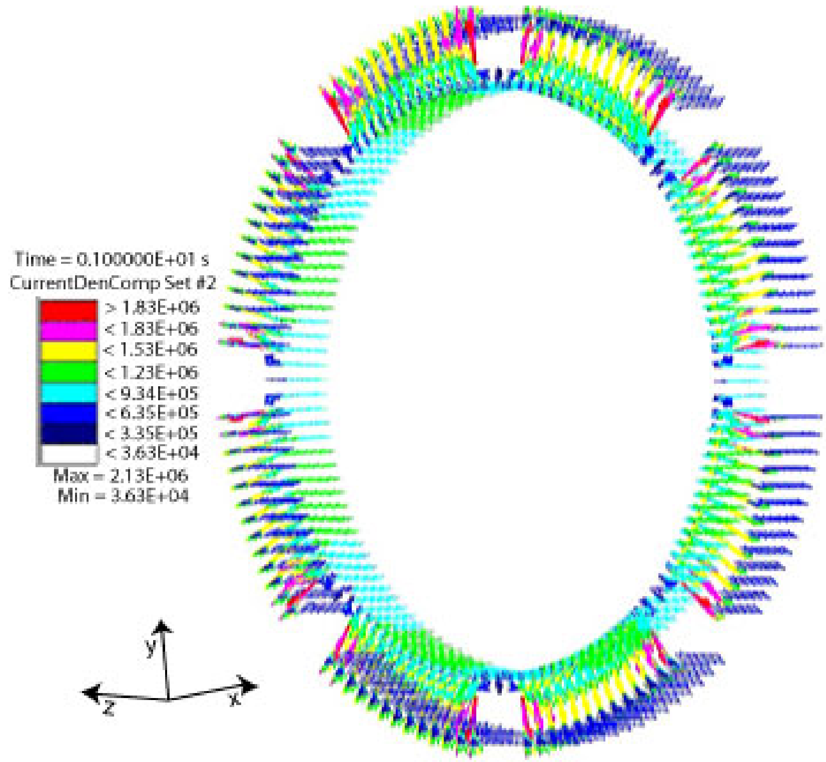


**Figure 7. Magnetic field distribution on a slip ring, brushes, and buses at 1.0 s for aspect ratio 1:3.**

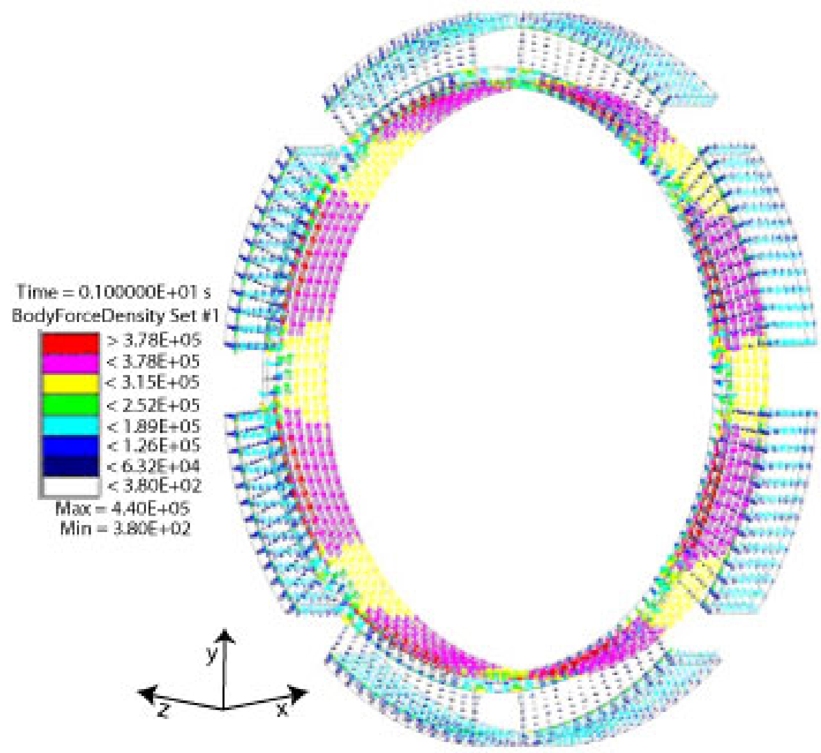


**Figure 8. Body force distribution on a slip ring, brushes, and buses at 1.0 s for aspect ratio 1:3.**

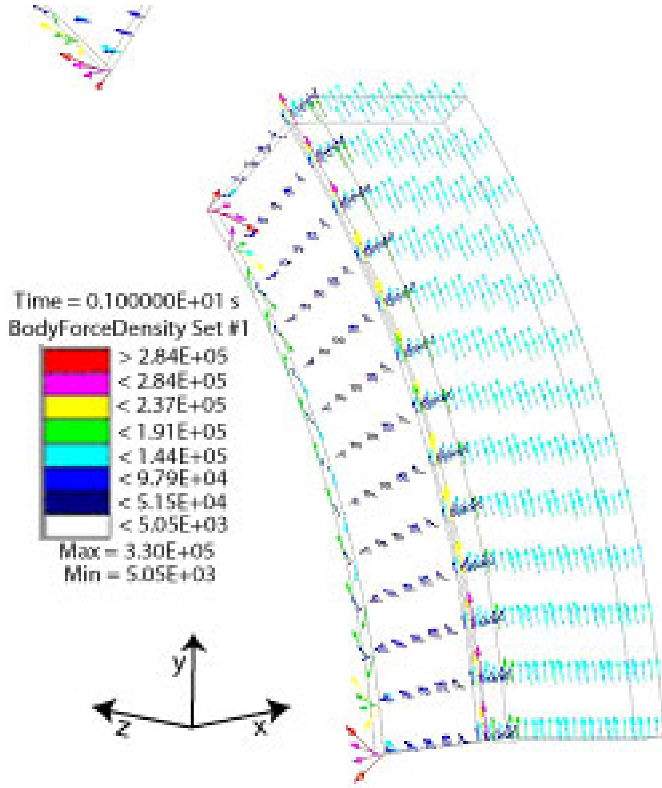


**Figure 9. Detailed body force distribution on a brush at 1.0 s for aspect ratio 1:3.**

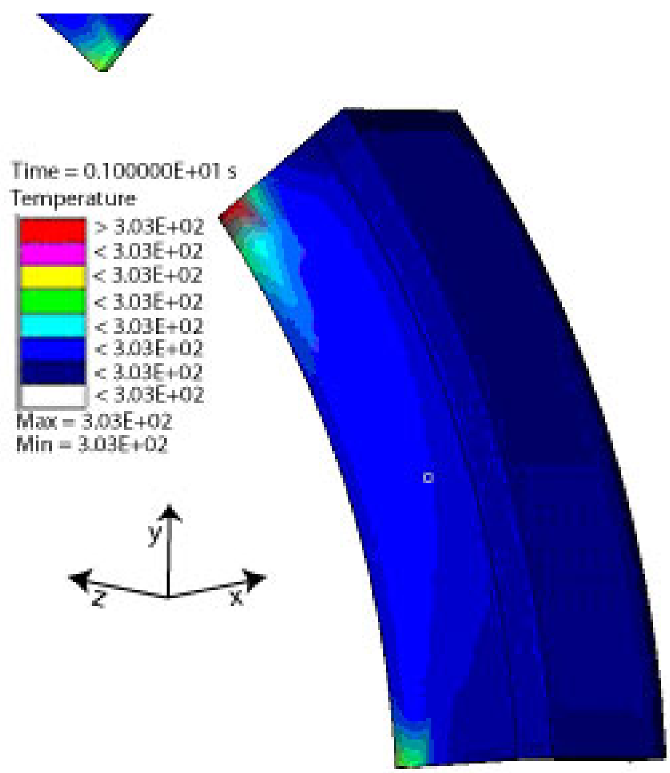


**Figure 10. Temperature distribution on a brush at 1.0 s for aspect ratio 1:3.**

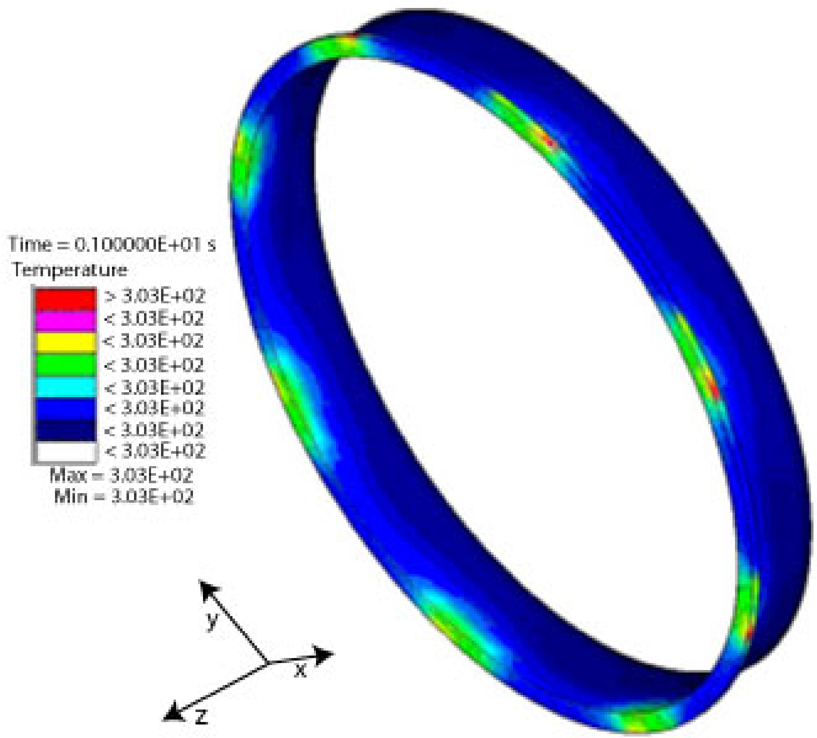


**Figure 11. Temperature distribution on a brush at 1.0 s for aspect ratio 1:3.**

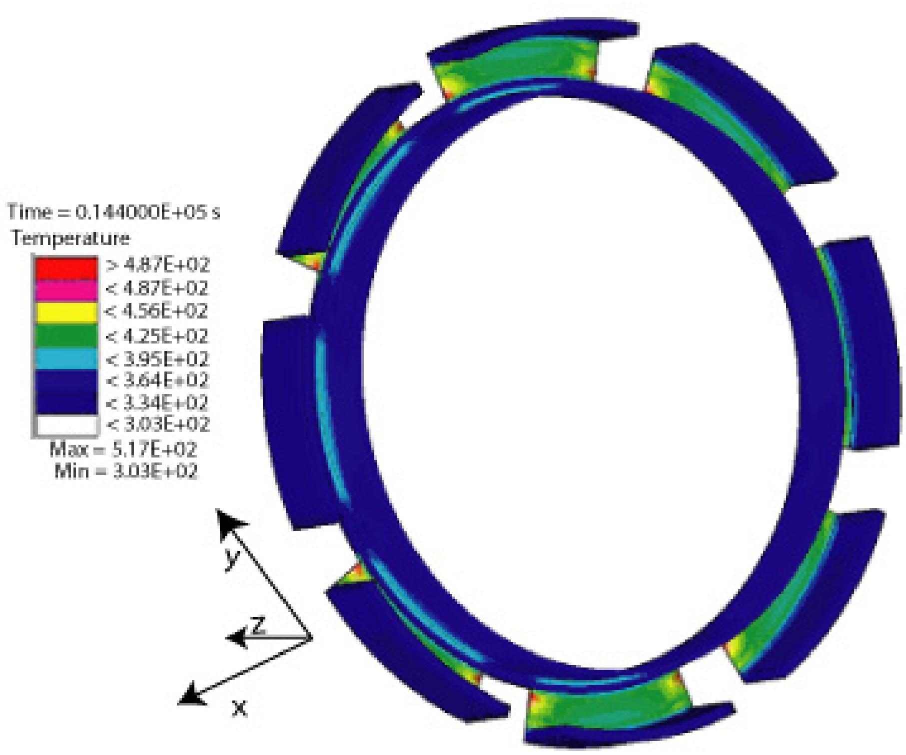


**Figure 12. Temperature distribution on a slip ring, brushes, and bus after 4 hours for aspect ratio 1:3.**

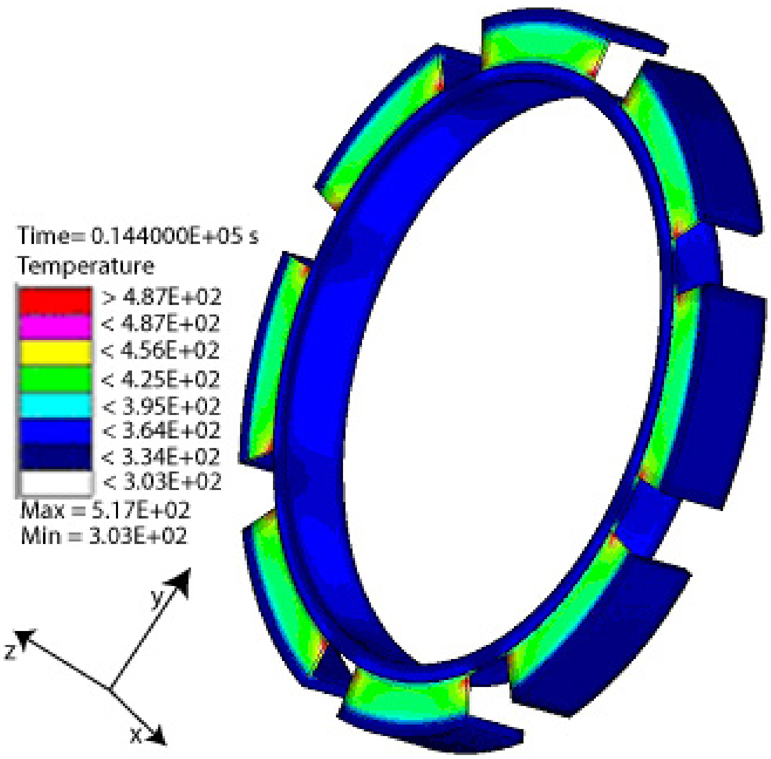


**Figure 13. Temperature distribution on a slip ring, brushes, and bus after 4 hours for aspect ratio 1:3.**

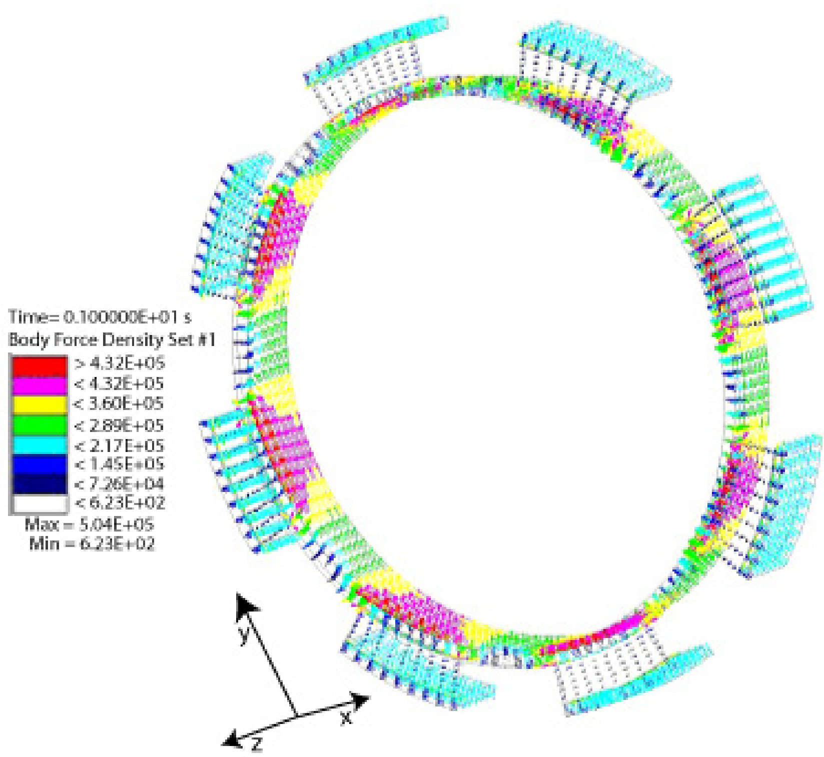


**Figure 14. Body force distribution on a slip ring, brushes, and buses at 1.0 s for aspect ratio 1:2.**

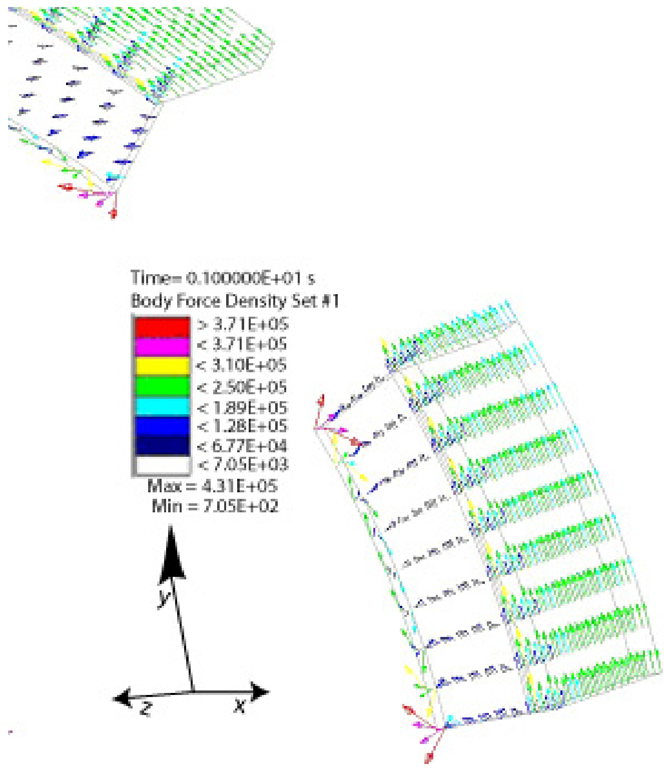


**Figure 15. Body force distribution on a brush at 1.0 s for aspect ratio 1:2.**

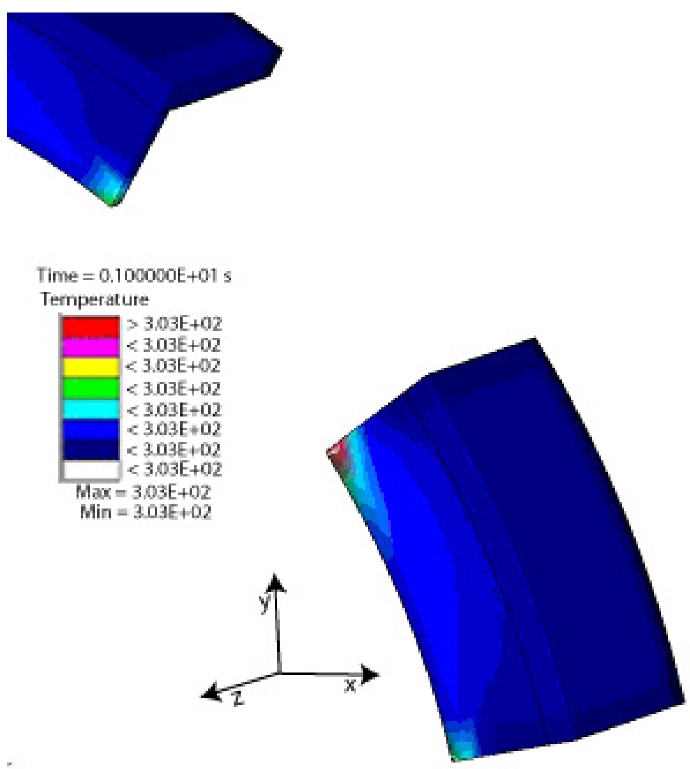


**Figure 16. Temperature distribution on a brush at 1.0 s for aspect ratio 1:2.**

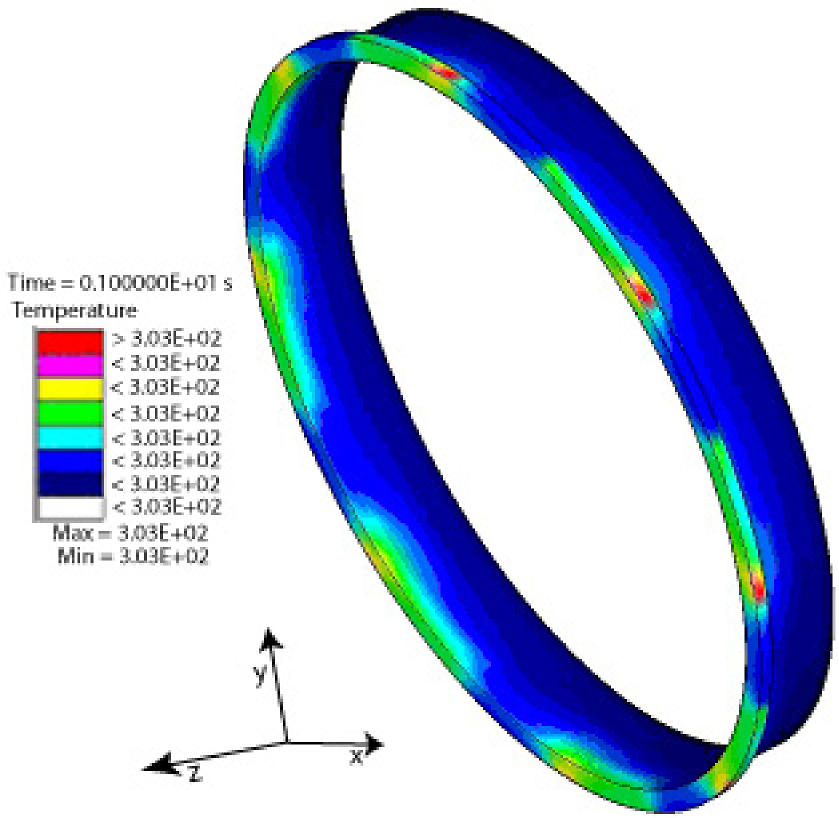


**Figure 17. Temperature distribution on a slip ring at 1.0 s for aspect ratio 1:2.**